ARTICLE NO. 79-0647R

Interior Noise Studies for Single- and Double-Walled Cylindrical Shells

Earl H. Dowell*
Princeton University, Princeton, N.J.

The modal theory of acoustoelasticity is applied to the determination of the sound levels caused by a prescribed external sound excitation which is transmitted through a cylindrical shell. A circumferential pseudo-traveling pressure wave excitation is studied as representative of a propeller sound field. It is shown how other excitations such as point mechanical loading, plane wave, and reverberation random may be synthesized by superposition of circumferential waves. Representative numerical results illustrate the importance of structural and acoustic frequency matching in the determination of interior sound levels and clarify the role of the cylindrical shell ring frequency. An exploratory study of a double-wall geometry is conducted.

I. Introduction

WITH the recent interest in fuel-efficient aircraft, the turboprop has received renewed attention. However, one of its potential disadvantages is a higher level of external and, hence, internal noise. For several years, Princeton, under grants from NASA Langley Research Center (NASA Grant NSG 1253), has been concerned with the response of structures to prescribed noise field. Recently, a theoretical model has been developed that is capable of predicting the interior noise for any structural model surrounding an acoustic cavity subjected to any prescribed exterior noise field.[1] Most recently, a computer code has been written and exercised to predict analytically the interior noise for cylindrical shell models of aircraft fuselage for prescribed harmonic (pure tone) exterior noise fields. Included in the theoretical model, as it has been developed, are: 1) detailed structural and interior space geometrical and sound-absorbing parameters; 2) pressurization; 3) a distributed pseudo-traveling wave acoustic loading representative of an exterior noise field due to a propeller; and 4) both open and closed cavity ends.

The structural wall and acoustic cavity are described in terms of their natural modes; hence, the analytical model is reduced to a system of acoustic-structural (acoustoelastic) spring-mass-damper oscillators.

In Sec. II, the basic analytical capability is described, including numerical results for a simple isotropic cylinder representation of a turboprop aircraft fuselage with a traveling wave exterior noise field. In Sec. III the model of Sec. II is simplified to consider a mechanical point excitation. Also considered in Sec. III is a uniform spatial excitation for its relevance to the discussion of Sec. IV. In Sec. IV, it is shown how a plane wave harmonic excitation may be represented as a summation of circumferential waves, thus allowing the analytical model of Sec. II to be used. No numerical results are presented for these cases; however, no difficulty is anticipated in modifying the existing computer code to obtain such numerical results. Also in Sec. IV, using the concepts of power spectral density and transfer function for sinusoidal inputs, it is shown how the basic analytical model of Sec. II may be used for a random exterior noise field. Again, the existing computer code may be extended to include random inputs. Section V contains the principal conclusions of the study.

Presented as Paper 79-0647 at the AIAA 5th Aeroacoustics Conference, Seattle, Wash., March 12-14, 1979; submitted March 23, 1979; revision received Jan. 7, 1980.

Index categories: Noise; Structural Dynamics.

*Professor, Mechanical and Aerospace Engineering. Associate Fellow AIAA.

II. Mathematical Analysis

The basic analytical approach as well as detailed mathematical results are described in Sec. II.A for a single isotropic cylindrical shell under a pseudo-traveling wave circumferential pressure load which represents the external pressure field due to a rotating propeller. The analysis is extended subsequently to include the effects of a double wall. The next stage in the development of the theoretical model would be to include the effects of rings and longitudinal stiffeners on the shell dynamics. When an orthotropic shell assumption will suffice, one need only replace the formula for the frequencies of an isotropic shell by its orthotropic counterpart.

In Sec. II.B, numerical results are presented for a representative baseline configuration. Convergence and trend studies are also reported.

Analysis

Our basic goal is to develop the equations of motion for two concentric cylindrical shells with a shallow annular cavity between them (double wall) and a large interior cavity (aircraft cabin). Any (specified) external pressure loading may be considered, although the primary focus is a circumferential pseudo-traveling wave loading representative of a propeller acoustic source.

In pursuing this goal, we consider a hierarchy of models with increasing realism, but also, increasing analytical complexity. These may be identified by their treatment of the structural cylindrical shells and the acoustic cavities. They are: 1) cylindrical shells: a) isotropic, b) orthotropic, c) discretely stiffened, and 2) acoustic cavities: a) inner cavity only, and b) inner and annular cavity. The theory of Ref. 1 and available results for cylindrical shells[2-4] and cylindrical acoustic cavities[5,6] are sufficient to allow us to write the equations of motion.

In the paper, the detailed equations of motion are written first for the simplest model—a single isotropic cylinder with a single cavity. Bhat and Mixson's model[7] (after Cockburn and Jolly[8]) for an open-ended cylindrical cavity is similar, except that the longitudinal acoustic modes may differ. Here we consider both closed- and open-ended cavities. Also, we allow for internal absorption material on the walls and ends of the cavity after Ref. 1.

We briefly indicate below how the more complete models can be constructed in detail.

1) Cylindrical shells:

b) orthotropic—simply requires a somewhat more elaborate formula for the structural natural frequencies.

c) discretely stiffened—as a preliminary, requires a Rayleigh-Ritz analysis for determining structural natural frequencies using, for example, the isotropic cylinder natural modes for the primitive modal expansion.

2) Acoustic cavities:

b) inner and annular cavity—the annular cavity is usually sufficiently shallow that only the lowest (uniform) radial mode is required. However, in general, this mode will couple the inner and outer cylindrical shells and these coupled modes will have to be computed. Subsequently, the double-wall geometry is considered in an exploratory fashion in this paper by ignoring the coupling between inner and outer cylindrical shells. It should be noted that from a standpoint of minimizing interior noise, it is desirable to have a double-wall design which minimizes this coupling. Hence, the simplified model which ignores the coupling may prove useful for design analysis.

See Ref. 1 for a complete list of symbols and the development of the following equations from fundamental principles.

Definitions

$$p=\rho_0 c_0^2 \sum_n (P_n F_n / M_n^A) \quad \text{acoustic pressure} \tag{1}$$

$$M_n^A \equiv \frac{\int F_n^2 \mathrm{d}V}{V} \quad \text{acoustic generalized mass} \tag{2}$$

$$w=\sum q_m \psi_m \quad \text{wall deflection} \tag{3}$$

$$M_m \equiv \int \psi_m^2 \mathrm{d}A \quad \text{wall generalized mass} \tag{4}$$

$$C_{nr} \equiv \frac{\int (F_n F_r / Z_a)\mathrm{d}A}{A_A} \quad \text{absorption coupling coefficient} \tag{5}$$

$$L_{nm} \equiv \frac{1}{A_F}\int F_n \psi_m \mathrm{d}A \quad \text{acoustoelastic coupling coefficient} \tag{6}$$

$$Q_m^E \equiv -\int p^E \psi_m \mathrm{d}A \quad \text{wall-generalized force} \tag{7}$$

Acoustic Modal Equation

$$\ddot{P}_n + \omega_n^{A2} P_n + \frac{A_A \rho_0 c_0^2}{V}\sum_r \frac{\dot{P}_r C_{nr}}{M_r^A} = -\sum_m \frac{A_F}{V} L_{nm} \ddot{q}_m \tag{8}$$

Wall Modal Equation

$$M_m[\ddot{q}_m + 2\zeta_m \omega_m \dot{q}_m + \omega_m^2 q_m] = \rho_0 c_0^2 A_F \sum_n P_n \frac{L_{nm}}{M_n^A} + Q_m^E$$

acoustoelastic coupling term (9)

The above formulation applies to any structural wall enclosing any acoustic cavity with any external excitation subject to broad assumptions of linearity and small perturbations.[1] We now turn to the specific geometry and loading shown in Fig. 1, i.e., a circular cylindrical shell with an external pressure load. The load is assumed to be simple-harmonic in time and is a pseudo-traveling wave in the circumferential direction. It is taken as constant over some limited span in the axial direction. The frequency and wavespeed are related to the propeller rpm and blade radius as follows. The frequency is equal to the blade rpm (in Hertz) times the number of blades. The wavespeed is equal to the frequency times the blade radius.

The determination of ω_n^A, ω_m is discussed separately in Appendices A and B. The natural modes are:

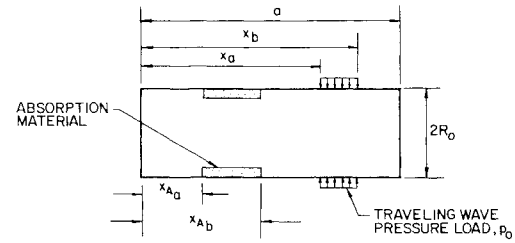

Fig. 1 Problem geometry.

$$\psi_m = \sin(m_x \pi x/a) \begin{matrix}\cos m_\theta \theta \\ \sin m_\theta \theta\end{matrix} \quad \text{structural}$$

$$F_n = \cos(n_x \pi x/a) J_{n_\theta}(k_{n_r n_\theta} r) \begin{matrix}\cos n_\theta \theta \\ \sin n_\theta \theta\end{matrix} \quad \text{acoustic}$$

The expression for F_n assumes a closed-end cylindrical cavity. For an open end, the cosine term in x is replaced by a sine function.

Pseudo-Traveling Wave Pressure Load

$$p^E = p_0 Re\ e^{i\omega[t-(R_0\theta/V)]} \tag{10}$$

$$= p_0 e^{i\omega t} \sum_{m_\theta=-\infty}^{\infty} C_{m_\theta} e^{i m_\theta \theta} \tag{11}$$

where V is the wavespeed and the Fourier coefficients are determined in the usual way as

$$C_{m_\theta} = \int_{-\pi}^{\pi} \frac{e^{-i m_\theta \theta - i\omega (R_0\theta/V)}}{2\pi}\mathrm{d}\theta = \frac{(-1)^{m_\theta}\sin\Omega\pi}{\pi(m_\theta+\Omega)}, \Omega \equiv \frac{\omega R_0}{V} \tag{12}$$

In Eq. (1) and hereafter, it is understood that the desired result is the real part of a complex number. Because of linearity, and orthogonality of the $e^{im\theta\theta}$, one may consider each term in Eq. (11) separately. Hence, by Fourier decomposition in θ, one reduces the number of spatial independent variables from r, x, θ to r, x. Thus, m_θ (from cylindrical structure) and n_θ (from cylindrical cavity) are the same. Both positive and negative m_θ are included. Note that Eq. (10) is not a classical traveling wave and, in particular, that p^E is discontinuous at $\theta=\pi$, $-\pi$. Of course, any external load can be expressed as a Fourier series, cf., Eq. (11), with appropriate coefficients C_{m_θ}.

Term Appearing in the Modal Equations

$$Q_m^E = -p_0 C_{m_\theta} e^{i\omega t}\int_{x_a}^{x_b} \sin\frac{m_x \pi x}{a}\mathrm{d}x(2\pi R_0) \tag{13}$$

$$L_{nm} = \frac{1}{a} J_{n_\theta}(k_{n_r n_\theta} R_0)\int_0^a \cos\frac{n_x \pi x}{a}\sin\frac{m_x \pi x}{a}\mathrm{d}x \cdot 2\pi R_0 \tag{14}$$

We assume that the absorption is uniform around the circumference for simplicity; otherwise, the circumferential cavity modes are coupled. Thus,

$$C_{nr} = \frac{1}{Z_a} J_{n_\theta}(k_{n_r n_\theta} R_0) J_{n_\theta}(k_{r_r n_\theta} R_0)\cdot 2\pi R_0 \cdot \int_{x_{A_a}}^{x_{A_b}} \cos\frac{n_x \pi x}{a}\cos\frac{r_x \pi x}{a}\mathrm{d}x \tag{15}$$

A similar calculation for absorption on one or both ends of the cylindrical cavity can be carried out.

$$M_m = \int_0^a \sin^2 \frac{m_x \pi x}{a} dx \cdot 2\pi R_0 = a/2 \cdot 2\pi R_0 \tag{16}$$

$$M_n^A = \int_0^a \int_0^{R_0} \cos^2 \frac{n_x \pi x}{a} J_{n_\theta}^2 (k_{n_r n_\theta} r) r dr dx 2\pi$$
$$= 2\pi R_0 \epsilon_{n_x} \frac{1}{2(k_{n_r n_\theta} R_0)^2} [(k_{n_r n_\theta} R_0)^2$$
$$- n_\theta^2] \cdot [J_{n_\theta} (k_{n_r n_\theta} R_0)]^2 \tag{17}$$

where

$$\epsilon_{n_x} = 1 \quad \text{for} \quad n_x = 0, \qquad \epsilon_{n_x} = \tfrac{1}{2} \quad \text{for} \quad n_x \geq 1$$

Steady-State Solution of Modal Equations

Neglecting the acoustoelastic coupling term in Eq. (9) (this should be a good assumption when one has enough absorption material to provide well-damped acoustic resonances,[1] a generally desirable design practice),

$$M_m [\ddot{q}_m + 2\zeta_m \omega_m \dot{q}_m + \omega_m^2 q_m] = Re Q_m^E e^{i\omega t}$$

Let

$$q_m = Re(q_m^R + i q_m^I) e^{i\omega t} \tag{18}$$

Then, solving Eq. (9) using Eq. (18) gives

$$q_m^R = \frac{Q_m^E}{M_m} \frac{(\omega_m^2 - \omega^2)}{[(-\omega^2 + \omega_m^2)^2 + (2\zeta_m \omega_m \omega)^2]}$$
$$q_m^I = \frac{Q_m^E}{M_m} \frac{2\zeta_m \omega_m \omega}{[(-\omega^2 + \omega_m^2)^2 + (2\zeta_m \omega_m \omega)^2]} \tag{19}$$

where m denotes a double subscript m_x and m_θ.

Using Eqs. (18) and (8) (neglecting coupling between acoustic modes due to absorption, which is reasonable for modest absorption[9]), one obtains

$$\ddot{P}_n + \omega_n^{A^2} P_n + \frac{A_A \rho_0 c_0^2}{V} \frac{\dot{P}_n C_{nn}}{M_n^A}$$
$$= +\omega^2 \sum_m L_{nm} \frac{A_F}{V} [q_m^R \cos\omega t - q_m^I \sin\omega t] \tag{20}$$

Let

$$P_n = Re[P_n^R + i P_n^I] e^{i\omega t} \tag{21}$$

Then, solving Eq. (20) using Eq. (21) gives

$$P_n^R = [+[-\omega^2 + \omega_n^{A^2}] \sum_m L_{nm} \omega^2 (A_F/V)$$
$$+ 2\zeta_n^A \omega_n^A \omega \sum_m L_{nm} q_m^I (A_F/V)] \Big/ ([-\omega^2 + \omega_n^{A^2}]^2 + 4\zeta_n^{A^2} \omega_n^{A^2} \omega^2) \tag{22a}$$

and

$$P_n^I = [+[-\omega^2 + \omega_n^{A^2}] \sum_m L_{nm} \omega^2 q_m^I (A_F/V)$$
$$- 2\zeta_n^A \omega_n^A \omega \sum_m L_{nm} q_n^R (A_F/V)] \Big/ ([-\omega^2 + \omega_n^{A^2}]^2 + 4\zeta_n^{A^2} \omega_n^{A^2} \omega^2) \tag{22b}$$

where

$$2\zeta_n^A \equiv \frac{\rho_0 c_0^2}{V} \frac{A_A C_{nn}}{\omega_n^A M_n^A}$$

and n denotes triple subscript n_r, n_x, and n_θ.

Calculation Procedure

Determine $\alpha_{n_r m_\theta} \equiv k_{n_r n_\theta} R_0$ from Ref. 6. See discussion in Appendix A.

Specify c_0, R_0, a.

Determine $\omega_n^{A^2} = c_0^2 [\frac{\alpha_{n_r n_\theta}^2}{R_0^2} + (\frac{n_x \pi}{a})^2]$.

Determine ω_m^2 from appropriate structural theory. See discussion in Appendix B.

Specify ω, V, and p_0. Determine C_{m_θ} from Eq. (12).

Specify $x_a \cdot x_b$. Determine Q_m^E from Eq. (13).

Determine L_{nm} from Eq. (14).

Specify x_{A_a}, x_{A_b}, Z_a. Determine C_{nr} from Eq. (15).

Determine M_m from Eq. (16).

Determine M_n^A from Eq. (17).

Specify ω_m. Determine q_m^R and q_m^I from Eq. (19) and w from Eq. (3).

Specify ζ_m^A. Determine P_n^R and P_n^I from Eq. (22) and p from Eq. (1).

Note the following relations hold:

Absorption Area:

$$A_A \equiv (x_{A_b} - x_{A_a}) 2\pi R_0$$

Flexible Wall Area:

$$A_F \equiv a 2\pi R_0$$

Cavity Volume:

$$V \equiv \pi R_0^2 a$$

To show this is so, one returns to Galerkin's method (or Rayleigh-Ritz) for the structure and Green's theorem for the acoustic cavity.[1] In both cases, one has the product of modes giving a quadratic form.

Double-Wall Analysis

Here we briefly outline the extension to a double-wall geometry; T denotes top or outer cylinder and B denotes bottom or inner cylinder.

The equations of motion are (cf., the above analysis and Ref. 1)

$$M_m^T [\ddot{q}_m^T + 2\zeta_m^T \omega_m^T \dot{q}_m^T + \omega_m^{T^2} q_m^T] = \rho_0 c_0^2 A_F^T \sum_n \frac{P_n L_{nm}^T}{M_n^A} + Q_m^E$$

outer cylinder (23)

$$M_m^B [q_m^B + 2\zeta_m^B \omega_m^B \dot{q}_m^B + \omega_m^{B^2} q_m^B] = -\rho_0 c_0^2 A_F^B \sum_n \frac{P_n L_{nm}^B}{M_m^A}$$

inner cylinder (24)

$$\ddot{P}_n + \omega_n^{A^2} P_n + \frac{A_A \rho_0 c_0^2}{V} \sum_r \dot{P}_r \frac{C_{nr}}{M_r^A} - \sum_m \frac{A_F^T}{V} L_{nm}^T \ddot{q}_m^T + \sum_m \frac{A_F^B}{V} L_{nm}^B q_m^B \quad \text{annular cavity between cylinders} \quad (25)$$

Premise: Except for $n_\theta = 0$ mode, there is very little acoustoelastic coupling.

Hence, a sequential solution may be used as follows:

1) Compute q_m^T (ignoring P_n and q_m^B) from Eq. (23).

2) Compute P_n (ignoring q_m^B) from Eq. (25).

Use

$$\omega_n^A \cong \frac{n_\theta}{(R_0 - d/2)} c_0, V \cong d2\pi(R_0 - d/2) \quad (26)$$

where d is the gap between the inner and outer walls. This should be accurate when $d/2\pi R_0 \ll 1$.

3) Compute q_m^B from Eq. (24).

Use

$$Q_m^{EB} \equiv -\rho_0 c_0^2 A_F^B \sum_n P_n \frac{L_{nm}^B}{M_n^A} \quad (27)$$

4) Using q_m^B from 3, iterate from 2, if necessary.

5) Compute interior sound field using q_m^B in the usual way, as in the analysis of a single-wall case.

Numerical Results

A computer program has been written to obtain solutions from this mathematical model. An example has been investigated and some highlights from the numerical results are discussed below. The following baseline parameters are used in the example (nominal case). See Refs. 10 and 11 for representative aircraft values.

Cylindrical shell (fuselage)	
material	aluminum
modulus of elasticity	10^7 psi
density	0.1 lb/in.^{3}
thickness	0.036 in.
radius	74 in.
length	180 in.
pressure differential	8.5 psi
Cavity (fuselage interior)	
speed of sound (air)	1117 ft/s
density (air)	0.002378 slug/ft^3
absorption material	
length of cylindrical shell covered	0-180 in.
impedance/characteristic air impedance	1
External pressure loading (traveling circumferential wave)	
magnitude	1 psi†
length of cylindrical shell covered	90-100 in.
propeller blade radius	60 in.
various frequencies (propeller rpm in Hz times number of blades)	
velocity of traveling wave pattern is taken equal to blade radius times frequency	

†1 psi is selected as an arbitrary reference. Because the theoretical model is linear, the cylindrical shell deflection and internal cavity pressure level are proportional to the magnitude of the external pressure loading. 1 psi = 170 dB.

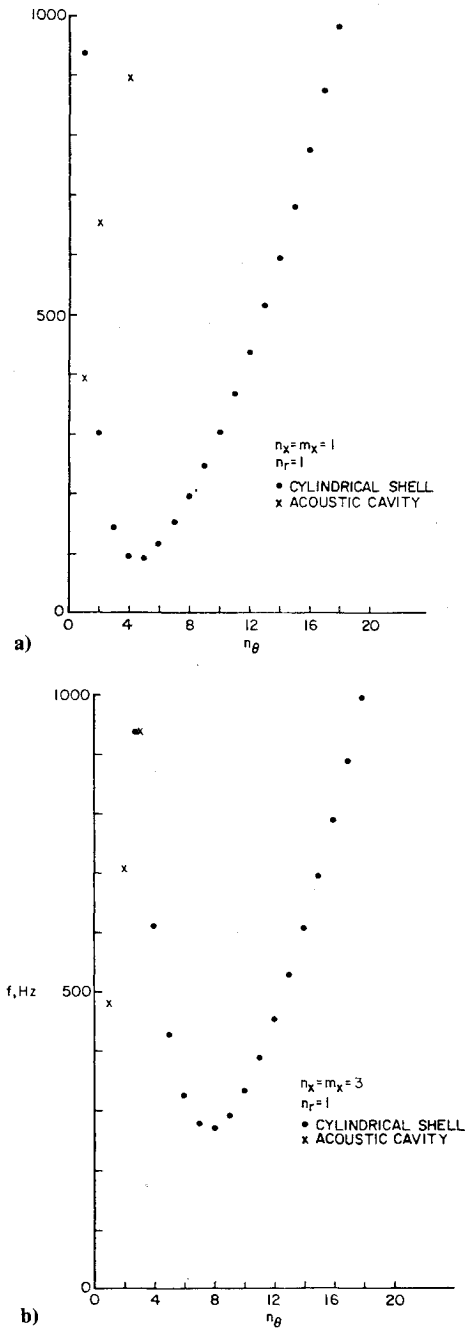

Fig. 2 Natural frequencies vs mode number. a) First axial mode; b) third axial mode.

Figures 2-5 show some of the important results obtained for this example. In Fig. 2, the natural frequencies of the cylindrical shell and acoustic cavity are plotted vs circumferential mode number n_θ. The first axial mode number of the cylindrical shell and the first axial and radial mode numbers of the acoustic cavity are shown in Fig. 2a, as these are the dominant ones. In Fig. 2b, analogous results for the third axial mode are also shown.‡ In the subsequent results shown in Figs. 4 and 5, the contributions of all of the first three axial and radial mode numbers are considered as well as all of the first 41 circumferential modes, $n_\theta = -40 \rightarrow +40$. Figure 2 allows one to anticipate the dominant circumferential modal contributions to the interior sound field. For example, one would expect the fundamental (lowest

‡The second axial mode proves less important than the third, presumably because the external load is near the fuselage center which is a node-line for this mode.

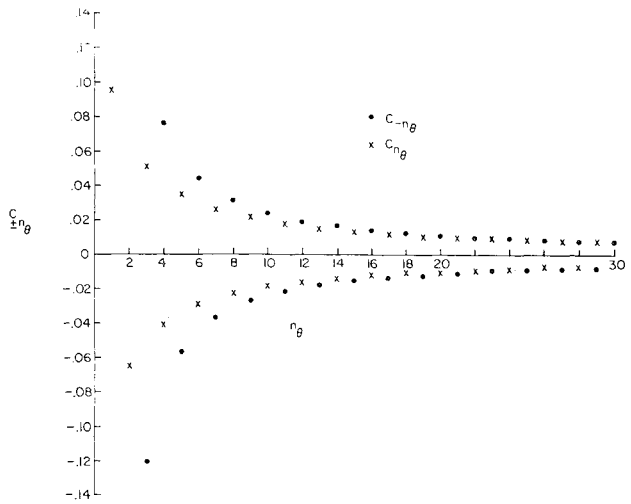

Fig. 3 Fourier coefficients of external pressure load.

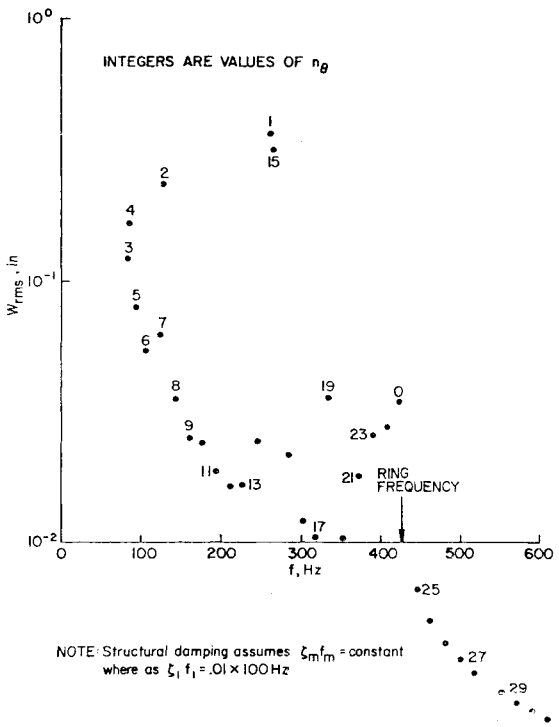

Fig. 4 Cylindrical shell deflection vs external pressure frequency.

frequency) shell mode to be important, in this case 82.8 Hz at $n_\theta = 4$. Also, one would expect significant sound levels when an acoustic and structural frequency are in close proximity for some n_θ, e.g., 2 and 3 and 90-139 Hz from Fig. 2a and, similarly, 290-330 Hz from Fig. 2b.

Another important indicator of a significant circumferential mode is the Fourier series representation of the traveling wave external pressure load. The Fourier coefficients of this series are shown in Fig. 3 for the present example. Two Fourier coefficients are shown for each value of $n_\theta = 0$ corresponding to the complex exponential representation of the pressure load [see Eq. (12)]. As can be seen, $n_\theta = 1$ makes the largest contribution to the external pressure load Fourier series. For large n_θ, the Fourier components decrease in inverse proportion to n_θ.

Now turn to Figs. 4 and 5. The spatial rms deflection and spatial rms internal pressure/external pressure magnitude are shown as a function of external pressure load frequency. The external pressure is simple-harmonic in time and travels about the cylindrical shell. Results were computed with the external

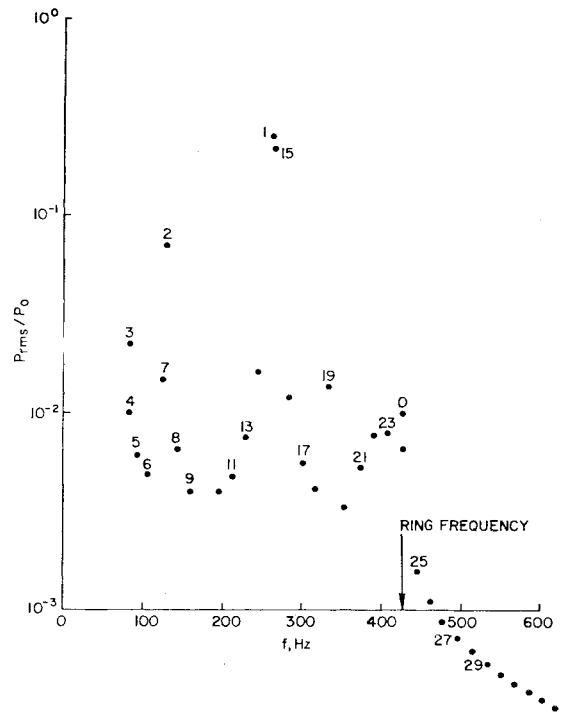

Fig. 5 Ratio of internal/external pressure vs external pressure frequency.

pressure frequency set to various structural resonant frequencies (corresponding to $n_\theta = 0 \rightarrow 34$ for $m_x = 1$) since this would be a maximum response condition. External excitation at acoustic resonant frequencies gives a smaller response for the absorption material used in the present example. As expected, the important circumferential modes identified from Figs. 2 and 3 do indeed lead to the largest structural deflections and internal sound levels in Figs. 4 and 5.

An important result is that for the above excitation, the ring structural frequency (423 Hz at $n_\theta = 0$), there is a rapid drop in structural and acoustic response levels. This is because structural and acoustic mode frequency mode matching or near matching is unlikely except at much higher frequencies. This result, however, may not carry over to stiffened cylindrical shells.

Another important conclusion, implicit in the above, is that for a single-frequency (pure tone) excitation, it will be relatively easy to identify the dominant modes in the response. However, for a near-resonant response condition, the response levels will be sensitive to small differences between the excitation and structural natural frequencies and thus difficult to predict accurately.

Convergence

A convergence study has been carried out for $f = 265.4$ Hz using various numbers of modes. The results are shown in Table 1. The results indicate that three radial modes and one axial mode give accurate results. The number of circumferential modes needed, of course, varies with excitation

Table 1 Convergence study

p_{rms}/p_0	$(n_r)_{max}$	$(n_x)_{max}$	$(n_\theta)_{max}$	$(m_x)_{max}$
0.254	3	3	9	3
0.254	3	3	9	1
0.238	3	1	9	1
0.113	1	3	9	1
0.248	5	1	9	1
0.106	1	1	9	1

$f = 265.4$ Hz baseline case (nominal)

Table 2 Effect of damping and pressure differential

$f = 265.4$ Hz, except as noted ($n_\theta = 1$ resonant frequency for $p = 8.5$ psi)	w_{rms}, in.	p_{rms}/p_0
Nominal	0.368	0.254
Change in structural damping form $\zeta = 0.01$ to 0.02	0.184	0.127
Change in pressure differential from $\Delta p = 8.5$ to 0 psi	0.252 0.373[a]	0.173 0.258[a]

[a] $f = 264.3$ Hz ($n_\theta = 1$ resonant frequency for $\Delta p = 0$ psi)

Table 3 Effect of open- vs closed-end and placement of absorption material

	p_{rms}/p_0
Nominal (closed end)	0.254
Open end	0.193
Absorption along cylinder and on ends	0.210
Absorption on ends only	0.351
$f = 265.4$ Hz baseline case	

frequency. The present results, which were obtained using up to 41 circumferential modes appear well-converged for the frequency range covered.

Trend Studies

Damping: The response at resonance is, as expected, inversely proportional to structural damping (see Table 2).

Pressure Differential: A loss of pressure differential can cause a significant reduction in response by detuning a structural response by changing the structural natural frequency. However, if the excitation frequency is retuned to the new natural frequency, the response will be increased (although only slightly in the example shown in Table 2).

Cavity End Conditions and Absorption: Table 3 compares the results from closed- and open-ended cylinders. Also shown is a comparison of results for various placements of absorption material. The results speak for themselves. In Fig. 6 results are shown for various portions of a cylindrical shell covered by absorption material. As expected, the structural response is insensitive to this parameter, but the interior noise levels decrease with an increase in absorption material.

External Pressure Load Extent: As expected and as shown in Fig. 7, the greater the extent of the external load distribution (for a given magnitude of pressure), the larger the structural response and interior noise.

Double Wall: A double-wall example has also been examined. The acoustoelastic coupling between the two walls has been ignored however. Except for the $n_\theta = 0$ mode, this should be satisfactory as long as the inner wall deflection is substantially less than the outer wall deflection.[1] Of course, this latter condition is exactly what one would like from the standpoint of good acoustical design. The physical parameters for the nominal case are those of the baseline model, except that the radius of the inner shell is 71 in. (hence the distance between inner and outer walls is 3 in.), there is no pressure differential across the inner wall, and the absorption material covers the outer shell walls and end, but the inner shell end only.

The various acoustic and structural natural frequencies are shown in Fig. 8. The inner and outer wall deflections are shown in Fig. 9 for various excitation frequencies (chosen to correspond to outer wall structural natural frequencies). Recall that in the present solution procedure it is assumed that

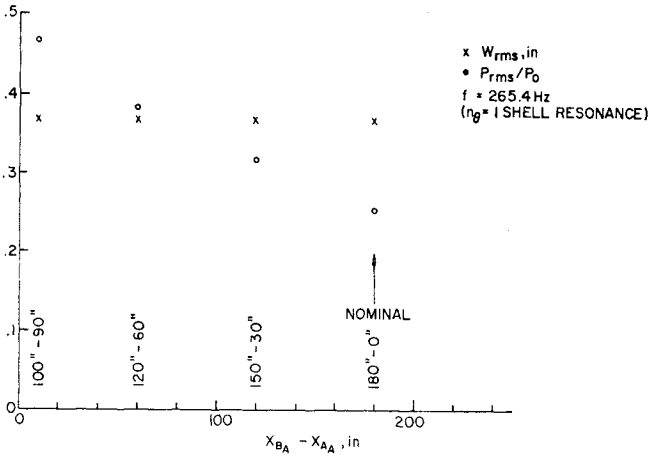

Fig. 6 Cylindrical shell deflection and internal sound pressure level vs length of cylinder covered by absorption material.

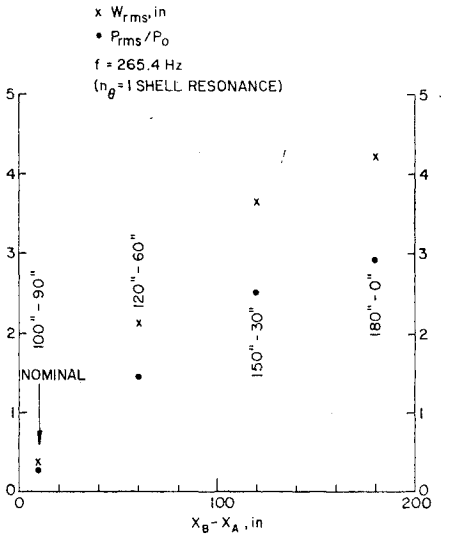

Fig. 7 Cylindrical shell deflection and internal sound pressure level vs length of cylinder covered by external pressure.

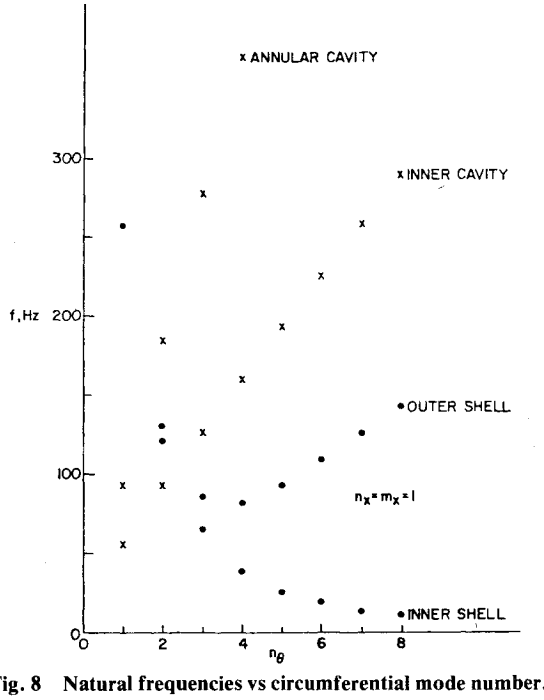

Fig. 8 Natural frequencies vs circumferential mode number.

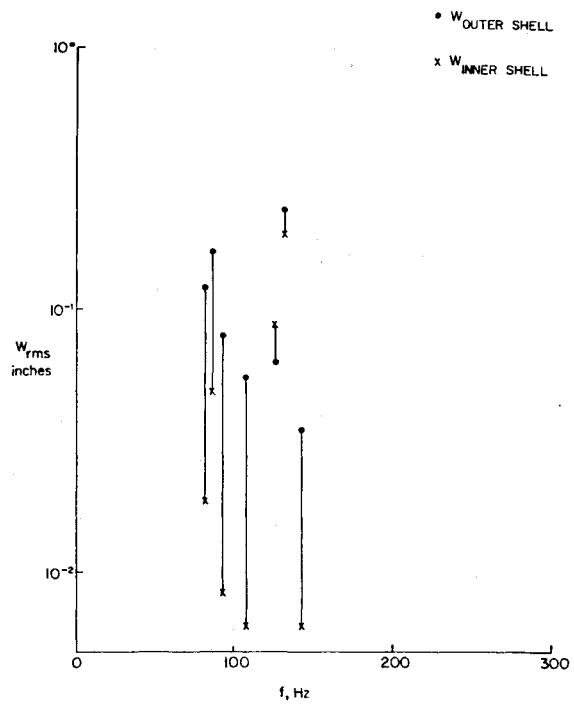

Fig. 9 Cylindrical shell deflections vs external pressure frequency.

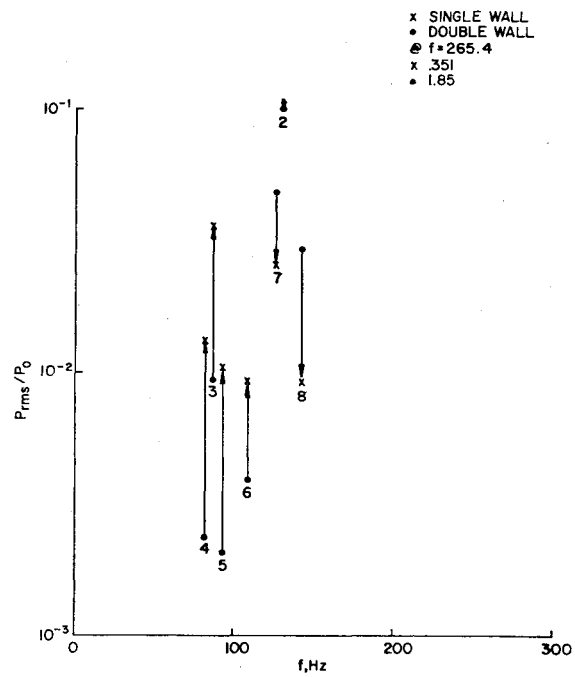

Fig. 10 Ratio of internal/external pressure vs external pressure frequency.

Table 4 Double wall design study

Case	f, Hz (n_θ)	rms w_T, in.	rms w_B, in.	p_{rms}/p_0
Nominal	82.77 (4)	0.121	0.189×10^{-1}	0.236×10^{-2}
	86.26 (3)	0.164	0.475×10^{-1}	0.943×10^{-2}
	93.64 (5)	0.789×10^{-1}	0.839×10^{-2}	0.207×10^{-2}
	108.89 (6)	0.544×10^{-1}	0.622×10^{-2}	0.390×10^{-2}
	125.56 (7)	0.622×10^{-1}	0.877×10^{-1}	0.491×10^{-2}
	130.34 (2)	0.233	0.190	0.101
	142.75 (8)	0.348×10^{-1}	0.625×10^{-2}	0.300×10^{-2}
	265.4 (1)	0.368	1.336	0.185×10^{-1}
	423.08 (0)	0.443×10^{-2}	0.343×10^{-2}	0.134×10^{-2}
Pressure differential on inner cylinder	11.49 (8)	0.387	0.111×10^{-3}	0.123×10^{-6}
	14.27 (7)	0.362	0.227×10^{-3}	0.302×10^{-6}
	18.86 (6)	0.313	0.585×10^{-3}	0.115×10^{-5}
	26.49 (5)	0.269	0.197×10^{-2}	0.852×10^{-5}
	39.93 (4)	0.234	0.883×10^{-2}	0.131×10^{-3}
	66.11 (3)	0.211	0.488×10^{-1}	0.43×10^{-2}
	124.4 (2)	0.248	0.376	0.213
	264.4 (1)	0.373	0.629	0.898
	422.8 (0)	0.438×10^{-1}	0.525×10^{-2}	0.155×10^{-2}
Pressure differential on inner cylinder $h_B=0.072$ in.	11.49 (8)	0.387	0.106×10^{-3}	0.794×10^{-7}
	14.27 (7)	0.361	0.212×10^{-3}	0.215×10^{-6}
	18.86 (6)	0.313	0.577×10^{-3}	0.968×10^{-6}
	26.49 (5)	0.269	0.197×10^{-2}	0.822×10^{-5}
	39.93 (4)	0.234	0.898×10^{-2}	0.133×10^{-3}
	66.11 (3)	0.211	0.537×10^{-1}	0.469×10^{-2}
	124.4 (2)	0.248	0.571	0.323
	264.3 (1)	0.373	0.365	0.525
	422.8 (0)	0.438×10^{-1}	0.241×10^{-2}	0.763×10^{-3}
Pressure differential on inner cylinder $h_B=0.072$ in., $d=6$ in.	124.4 (2)	0.248	0.472	0.302
	264.3 (1)	0.373	0.212	0.355
	422.8 (0)	0.438×10^{-1}	0.320×10^{-2}	0.104×10^{-2}
Pressure differential on inner cylinder, $d=6$ in.	124.4 (2)	0.248	0.719	0.460
	264.3 (1)	0.373	0.386	0.646
	422.8 (0)	0.438×10^{-1}	0.508×10^{-2}	0.165×10^{-2}
Pressure differential on inner cylinder, $d=6$ in., $\rho_B=0.05$ lb/in.^{3}	124.4 (2)	0.248	0.473×10^{-1}	0.307×10^{-1}
	264.3 (1)	0.373	0.321×10^{-1}	0.534×10^{-1}
	422.8 (0)	0.438×10^{-1}	0.815×10^{-3}	0.366×10^{-3}
Pressure differential on inner cylinder, $d=6$ in., $\rho_B=0.2$ lb/in.^{3}	124.4 (2)	0.248	0.264×10^{-1}	0.164×10^{-1}
	264.3 (1)	0.373	0.183×10^{-1}	0.311×10^{-1}
	422.8 (0)	0.438×10^{-1}	0.361×10^{-1}	0.106×10^{-3}

the inner shell deflections are much less than the outer shell deflections. Clearly, not all results in Fig. 9 satisfy this requirement, e.g., $f=125$ Hz. As one would expect in such a case, the interior acoustic pressure is larger for the double-wall geometry than for the single wall. See Fig. 10, where the double- and single-wall results are compared. Hence, for such an excitation frequency, a double wall actually makes matters worse.

At least in retrospect this behavior can be explained by reference to Fig. 8. There we see that near $f=125$ Hz the inner (bottom) and outer (top) walls have very close natural frequencies as does the inner cavity. Clearly, this would be a bad design if the excitation frequency is near $f=125$ Hz.

Design Analysis for a Double Wall

A simple example of how one might use the present analytical model in a design procedure has been carried out. The results are presented in Table 4. Several cases are considered in turn; in each case, the exciting frequencies are set equal to the outer cylinder resonant frequencies for the first axial mode, $m_x=1$, and the $n_\theta=0$ to $n_\theta=8$ circumferential modes. In an actual design study, one would need to insure that all circumferential and axial modes are included in the anticipated range of the excitation frequencies.

The spatial rms top w_T and bottom w_B cylinder deflections and inner cavity pressure p_{rms} are given in Table 4. Case 1 is the nominal one previously studied. The second case is for the pressure differential applied to the inner (bottom) rather than outer (top) cylinder. As may be seen, Case 2 has generally lower interior sound levels. Case 3 is for a doubling for the inner cylinder thickness and again the effect is generally favorable. Case 4 doubles the gap distance between cylinders and again the effect is favorable. For brevity, only the $n_\theta=0$, 1, 2 resonant frequencies are considered. Case 5 returns the inner thickness to its original smaller value, $h_B=0.036$ in., and here, as expected, the effect is to increase the interior sound level. Case 6 decreases the inner cylinder mass by a factor of two, but maintains the same stiffness level (in practice, this would be achieved by a stiffened shell geometry) and the effect is dramatically favorable. A doubling of the inner cylinder mass, Case 7, is also dramatically favorable.

In all the above cases, it is of interest to note that where low interior sound levels are achieved, the inner cylinder deflection is much smaller than the outer cylinder deflection. In simple terms, if this is not true, it is better not to have an inner cylinder at all! Also, all of the preceding results are consistent with the hypotheses that 1) for two cylinders of comparable properties, it is more effective to stiffen (by pressure differential or increase thickness) the inner cylinder rather than the outer one and 2) is it very effective to separate (detune) the inner and outer cylinders by changing their resonant frequencies, e.g., by mass changes.

III. Mechanical Point Excitation and Uniform Spatial Excitation

These simpler excitations are of interest because they allow a more direct experimental assessment of any theoretical model and also serve as building blocks for more complex random excitations. See the discussion in Sec. IV with respect to the latter.

Mechanical Point

A mechanical point excitation can be represented by

$$p^E=F_0\delta(x-x_F)\delta(R_0\theta)e^{i\omega t} \tag{28}$$

where F_0 is the point force magnitude, δ is a delta function, and $x=x_F$, $\theta=0$ is the location of the point force.

This point force itself may be expressed as a summation of traveling waves as follows:

$$p^E=F_0\delta(x-x_F)e^{i\omega t}\sum_{}^{\infty}C_m e^{im_\theta\theta} \qquad m_\theta=-\infty,\infty \tag{29}$$

where $C_{m_\theta}=1$ for all m_θ

Thus, the generalized force needed for the analysis of Sec. II is:

$$Q_m^E=-2\pi F_0 C_{m_\theta}\sin\frac{m_x\pi x_F}{a}e^{im_\theta\theta}e^{i\omega t} \tag{30}$$

Uniform Spatial

A uniform spatial excitation can be represented by

$$p^E=p_0 Re\{e^{i\omega t}\} \tag{31}$$

This may be expressed as a summation of traveling waves as follows:

$$p^E=p_0 e^{i\omega t}\sum_{}^{\infty}C_{m_\theta}e^{im_\theta\theta} \qquad m_\theta=-\infty,\infty \tag{32}$$

where $C_{m_\theta}=1$ for $m_\theta=0$ and is otherwise zero. Thus the generalized force needed for the analysis of Sec. II is:

$$Q_m^E=-2\pi R_0 p_0\frac{[1-\cos m_x\pi]}{m_x\pi}a \tag{33}$$

Hence, the uniform spatial excitation is also treatable by the method of Sec. II.

Numerical results have been obtained but are omitted for the sake of brevity.

IV. Plane Wave and Idealized Reverberation Random Driving Forces

The response to a sinusoidal excitation, either circumferential waves or point excitation, may be used as a basic building block to construct responses for these two types of driving forces.

Plane Wave

Denote Cartesian coordinates by x,y,z and polar coordinates by r,θ,z, where z is the axis along the centerline of the cylindrical shell. A plane wave pressure along the x axis can be represented by

$$p_p=p_0\exp[i\omega(x-c_0t)/c_0] \tag{34}$$

or, in polar coordinates,

$$p_p=p_0\exp[i\omega(r\cos\theta-c_0t)/c_0] \tag{35}$$

where ω is the frequency of the incoming wave, c_0 the speed of sound, and p_0 the wave magnitude. Following Morse and Ingard,[5] the latter may be expressed as a Bessel-Fourier series.

$$p_p=p_0[J_0(kr)+\sum_{m=1}^{\infty}i^m\cos m\theta J_m(kr)]e^{i\omega t} \tag{36}$$

where $k\equiv\omega/c_0$ and $m=m_\theta$.

The total pressure acting on the cylindrical shell is the sum of the preceding incoming wave and the scattered wave. After some mathematical analysis, it is shown in Ref. 5 that the scattered wave pressure is given by

$$p_s=\sum_{m=0}^{\infty}A_m[J_m(kr)+iN_m(kr)]\cos m\theta e^{-i\omega t} \tag{37}$$

where

$$A_0 = \frac{p_0 J_1(kR_0)}{[J_1(kR_0) + iN_1(kR_0)]}$$

$m \neq 0$:

$$A_m = \frac{2i^m p_0 [J_{m+1}(kR_0) - J_{m-1}(kR_0)]}{[J_{m+1}(kR_0) - J_{m-1}(kR_0) + iN_{m+1}(kR_0) - iN_{m-1}(kR_0)]}$$

The total pressure acting on the cylindrical shell is thus

$$p^E = p_p + p_s \quad \text{at} \quad r = R_0 \tag{38}$$

This assumes that the cylindrical shell motion does not significantly affect the scattered wave. This assumption may be worthy of further study.

p^E is now expressed by Eqs. (3-5) as a sum of circumferential waves, and the analysis is thus reduced to the case previously treated in Sec. II. It will be of interest to consider responses with and without the scattered wave included to determine the significance of its effect.

Idealized Reverberation Random

Here is considered an exterior noise field which is uniform in space and random in time. From the basic theory of random processes,[12] it is known that

$$\Phi_{ww}(x,\theta;\omega) = |H_{wp}(x,y;\omega)|^2 \Phi_{pp}(\omega) \tag{39}$$

where Φ_{ww} is the power spectral density of the deflection at point x, θ; $\Phi_{pp}(\omega)$ is the power density of the pressure due to the exterior idealized reverberation random noise field; and H_{wp} is the transfer function which is the response to a unit exterior sound pressure that is distributed uniformly in space and is sinusoidal with frequency ω in time. An expression similar to Eq. (6) can be written with the interior sound field pressure replacing the cylindrical shell deflection.

The transfer functions needed to compute the interior sound field (and cylindrical shell deflection) are precisely those responses discussed in Secs. II and III for a uniform-in-space and sinusoidal-in-time exterior sound field.

V. Concluding Remarks

1) The feasibility of conducting low-frequency (below 1000 Hz) noise studies using structural and acoustic modal analysis has been demonstrated. Any prescribed external pressure excitation may be treated. A circumferential wave excitation was given special attention because of its ability to model a propeller noise field and also because it may serve as a basic Fourier building block for representing other external sound fields including point, plane wave, and random excitation.

2) The interior noise levels calculated can be explained by reference to matching or mismatching of exciting and structural/acoustic natural frequencies. A knowledge of the circumferential Fourier components of the external load is also useful and important in anticipating and/or interpreting the results.

3) Double walls are not necessarily beneficial, though it is the exceptional excitation frequency where they lead to an increase in interior noise levels.

4) For (pure tone) single-frequency external excitation, it will be difficult to predict interior noise levels accurately due to sensitivity of the results to small differences between excitation and structural/acoustics natural frequencies for near-resonant response conditions. However, the analytical model should still be useful in making qualitative design changes and decisions and providing insight and understanding in planning and interpreting experiments.

5) In design analysis, the method might proceed as follows. From a knowledge of the excitation frequencies, and principal circumferential harmonics, the most important acoustic cavity and structural modes are identified. A worst case assumption is made and the interior noise levels are calculated by equating the excitation frequency to the structural and acoustic resonant frequencies in the frequency range of interest. If noise levels are excessive, then acoustic absorption is added to suppress responses at acoustic resonances or structural mass, stiffness or damping is added to suppress response at structural resonances. Double-wall effects may also be helpful.

Appendix A: Acoustic Natural Modes of Cylindrical Cavities

$$\nabla^2 p + (\omega/c)^2 p = 0 \tag{A1}$$

Assume

$$p(r,\theta,x) = R(r)\Theta(\theta)X(x) \tag{A2}$$

Then,

$$X = \cos\frac{n_x \pi x}{a}, \quad n_x = 0,1,2,\ldots \tag{A3}$$

from

$$\left.\frac{dX}{dx}\right|_{x=0,a} = 0 \qquad \text{(rigid ends)}$$

and

$$\Theta = \frac{\sin n_\theta \theta}{\cos n_\theta \theta}, n_\theta = 0,1,2,\ldots \tag{A4}$$

from the periodicity requirement for p in θ and

$$R = AJ_{n_\theta}(k_{n_r} r) + BY_{n_\theta}(k_{n_r} r) \tag{A5}$$

with

$$(\omega/c_0)^2 = k_{n_r}^2 + \left(\frac{n_x \pi}{a}\right)^2 \tag{A6}$$

From boundary conditions on R, the eigenvalues of k_{n_r} are determined and, hence, the eigenfrequencies from Eq. (A6).

Complete Cylindrical Cavity

We require that $B = 0$ in Eq. (A5) so that R is bounded at $r = 0$. The other boundary condition is that

$$\left.\frac{\partial R}{\partial r}\right|_{r=R_0} = 0 \rightarrow J'_{n_\theta}(k_{n_r} R_0) = 0 \tag{A7}$$

The roots of Eq. (A7) define the $k_{n_r n_\theta}$.

Annular Cylindrical Cavity

The two boundary conditions are

$$\left.\frac{\partial R}{\partial r}\right|_{r=R_0,R_i} = 0$$

from which the eigenvalue equation is obtained, i.e.,

$$J'_{n_\theta}(k_{n_r} R_0) Y'_{n_\theta}(k_{n_r} R_i) - J'_{n_\theta}(k_{n_r} R_i) Y'_{n_\theta}(k_{n_r} R_0) = 0 \tag{A8}$$

The roots of Eq. (A8) are $k_{n_r n_\theta}$ (see Ref. 13).

The cavity pressure is now expressed as

$$p=\rho_0 c_0^2 \sum_n \frac{P_n F_n(r,\theta,x)}{M_n^A} \tag{A9}$$

where

$$M_n^A=\frac{1}{V}\int F_n^2 \mathrm{d}V=\frac{1}{\pi R_0^2 a}\int F_n^2 r\mathrm{d}r\mathrm{d}\theta\mathrm{d}x \tag{A10}$$

and for a complete cavity with rigid ends

$$F_n=J_{n_\theta}(k_{n_r n_\theta} r)\begin{matrix}\cos n_\theta\theta \\ \sin n_\theta\theta\end{matrix}\cos\frac{n_x x}{a} \tag{A11}$$

Appendix B: Structural Natural Modes of Cylindrical Shells

From Refs. 2-4, one may obtain expressions for the natural frequencies ω_m and modal functions ψ_m of a cylindrical shell. The latter are:

$$\psi_m=\sin\frac{m_x\pi x}{a}\begin{matrix}\cos m_\theta\theta \\ \sin m_\theta\theta\end{matrix}$$

where $m_x=1,2,3,4,\ldots$ and $m_\theta=0,1,2,3,\ldots$.

The former may be determined by several different available shell theories. Two are considered here. The first, and simpler, of these is the Donnell shell theory. It is accurate for m_θ sufficiently large and, indeed, is often used for all m_θ other than $m_\theta\equiv 1$, including $m_\theta\equiv 0$. For $m_\theta=1$, Donnell's theory is known to give less accurate results.[2-4] The expression for ω_m is[2]:

$$\left(\frac{R_0\omega_m}{c_{\mathrm{ref}}}\right)^2=(1-\nu^2)\alpha^4/(\alpha^2+m_\theta^2)^2+(\delta^2/12)(\alpha^2+m_\theta^2)^2 + \frac{\Delta p}{E\delta}(1-\nu^2)\left[\frac{\alpha^2}{2}+m_\theta^2\right] \tag{B1}$$

where

$$\alpha\equiv\frac{m_x\pi R}{a},\qquad \delta\equiv h/R_0,\qquad c_{\mathrm{ref}}^2\equiv\frac{E}{\rho_m(1-\nu^2)}$$

and R_0 is the shell radius, h the shell thickness, E the modulus of elasticity, ρ_m the shell density, ν is Poisson's ratio, and Δp is the static pressure differential (positive when interior pressure is larger than exterior).

There are numerous other, more accurate, shell theories which differ somewhat in detail, but are broadly similar. Among these, the theory associated with the name of Goldenvieser is discussed here. The value of $(R_0\omega_m/c_{\mathrm{ref}})$ is calculated from roots of the following determinant[2]

$$\begin{vmatrix} A & B & C \\ -B & D & E \\ -C & E & F \end{vmatrix}=0 \tag{B2}$$

where

$$A\equiv-\alpha^2-m_\theta^2[(1-\nu)/2]+\left(\frac{R_0\omega_m}{c_{\mathrm{ref}}}\right)^2$$

$$B\equiv-i[(1+\nu)/2]\alpha m_\theta$$

$$C\equiv-i\nu\alpha$$

$$D\equiv-m_\theta^2-\alpha^2[(1-\nu)/2] + (\delta^2/12)\{-2(1-\nu)\alpha^2-m_\theta{}^2\}+\left(\frac{R_0\omega_m}{c_{\mathrm{ref}}}\right)^2$$

$$E\equiv-m_\theta+(\delta^2/12)\{-(2-\nu)\alpha^2 m_\theta-m_\theta{}^3\}$$

$$F\equiv-1-(\delta^2/12)\{\alpha^2+m_\theta^2\}^2+\left(\frac{R_0\omega_m}{c_{\mathrm{ref}}}\right)^2 - \frac{\Delta p}{E\delta}(1-\nu^2)\left[\frac{\alpha^2}{2}+m_\theta^2\right]$$

Equations (B1) or (B2) may be used to compute the ω_m which are needed in the text depending upon the accuracy required. In the numerical examples of the present paper, Eq. (B1) was used.

Acknowledgment

The author would like to thank the reviewers for several helpful suggestions.

References

[1] Dowell, E.H., Gorman, G.F. III, and Smith, D.A., "Acoustoelasticity: General Theory, Acoustic Natural Modes and Forced Response to Sinusoidal Excitation, Including Comparisons with Experiment," *Journal of Sound and Vibration*, Vol. 52, June 1977, pp. 519-542.

[2] Dowell, E.H., "Flutter of Infinitely Long Plates and Shells, Part II: Cylindrical Shell," *AIAA Journal*, Vol. 4, Sept. 1966, pp. 1510-1518.

[3] Voss, H.M., "The Effect of an External Supersonic Flow on the Vibration Characteristics of Thin Cylindrical Shells," *Journal of Aerospace Sciences*, Vol. 28, Dec. 1961, pp. 945-956.

[4] Leissa, A.W., "Vibrations of Shells," SP-288, NASA 1973.

[5] Morse, P.M. and Ingard, K.U., *Theoretical Acoustics*, McGraw-Hill Book Co., Inc., New York, 1968.

[6] Abramowitz, M. and Stegun, I.A., *Handbook of Mathematical Functions*, National Bureau of Standards, Washington, D.C., 1964.

[7] Bhat, R.B. and Mixson, J.S., "Interior Noise in a Propeller-Driven Aircraft with a Cylindrical Fuselage," presented at the 94th Meeting of the Acoustical Society of America, Miami Beach, Fla., Dec. 1977.

[8] Cockburn, J.A. and Jolly, A.C., "Structural-Acoustic Response Noise Transmission Losses and Interior Noise Levels of an Aircraft Fuselage Excited by Random Pressure Fields," AFFDL-TR-68-2, Aug. 1968.

[9] Dowell, E.H., "Reverberation Time, Absorption and Impedance," *Journal of the Acoustical Society of America*, Vol. 64, July 1978, pp. 181-191.

[10] Wilby, J.F., "An Approach to the Prediction of Airplane Interior Noise," AIAA Paper 76-548, Palo Alto, Calif., July 1976.

[11] Bhat, W.V. and Wilby, J.F., "Interior Noise Radiated by an Airplane Fuselage Subjected to Turbulent Boundary Layer Excitation and Evaluation of Noise Reduction Treatments," *Journal of Sound and Vibration*, Vol. 18, Oct. 1971, pp. 449-464.

[12] Lin, Y.K., *Probalistic Theory of Structural Dynamics*, McGraw-Hill Book Co., Inc., New York, 1967.

[13] Hildebrand, F.B., *Advanced Calculus for Engineers*, Prentice-Hall, New Jersey, 1961, p. 576.